

Robustness and Independence of the Eigenstates with respect to the Boundary Conditions across a Delocalization-Localization Phase Transition

Zi-Yong Ge^{1,2} and Heng Fan^{1,2,3,4,*}

¹*Beijing National Laboratory for Condensed Matter Physics,*

Institute of Physics, Chinese Academy of Sciences, Beijing 100190, China

²*School of Physical Sciences, University of Chinese Academy of Sciences, Beijing 100190, China*

³*CAS Center for Excellence in Topological Quantum Computation, UCAS, Beijing 100190, China*

⁴*Songshan Lake Materials Laboratory, Dongguan 523808, China*

(Dated: July 8, 2022)

We focus on the many-body eigenstates across a localization-delocalization phase transition. To characterize the robustness of the eigenstates, we introduce the eigenstate overlaps \mathcal{O} with respect to the different boundary conditions. In the ergodic phase, the average of eigenstate overlaps $\bar{\mathcal{O}}$ is exponential decay with the increase of the system size indicating the fragility of its eigenstates, and this can be considered as an eigenstate-version butterfly effect of the chaotic systems. For localized systems, $\bar{\mathcal{O}}$ is almost size-independent showing the strong robustness of the eigenstates and the broken of eigenstate thermalization hypothesis. In addition, we find that the response of eigenstates to the change of boundary conditions in many-body localized systems is identified with the single-particle wave functions in Anderson localized systems. This indicates that the eigenstates of the many-body localized systems, as the many-body wave functions, may be independent of each other. We demonstrate that this is consistent with the existence of a large number of quasilocal integrals of motion in the many-body localized phase. Our results provide a new method to study localized and delocalized systems from the perspective of eigenstates.

I. INTRODUCTION

Recently, understanding the mechanisms of thermalization and localization in an isolated quantum many-body systems has been attracted many interests. Generally, for a closed quantum many-body system, starting from a far-from-equilibrium initial state, the system can always thermally equilibrate under an unitary evolution [1–5]. We call these systems as ergodic systems, and the microscopic mechanism of this thermalization is known as eigenstate thermalization hypothesis (ETH). Nevertheless, there also exist the localized systems, which are the typical examples violating ETH [6]. The localized systems are first identified by Anderson in a non-interacting fermion system with impurity scatterings, which is dubbed Anderson localization (AL) [7]. In recent two decades, it was shown that the localization can persist in the presence of interactions, which is now termed many-body localization (MBL) [8–14]. Benefiting from the experimental advances of synthetic quantum many-body systems, the MBL has been realized in various of platforms, such as optical lattice [15–17], nuclear magnetic resonance [18], trapped ions [19], and superconducting circuits [20, 21].

Comparing with ergodic and AL systems, the MBL systems posses many unique properties. For the dynam-

ics, the MBL system can hardly be thermalized due to the existence of a large number of quasi-local integral of motions [22, 23], and the entanglement entropies can exhibit long-time logarithmic spreading [24, 25], while the growth of entanglement is ballistic in the ergodic systems [26]. Additionally, according to the level statistics, it is shown that the spectrum of the MBL systems obey Poisson distribution, while it is Wigner-Dyson distribution in the ergodic phase [9, 11, 27–29]. Furthermore, the eigenstates of MBL systems also have many unique properties, especially the entanglement. It is shown that the eigenstates of the MBL systems have low entanglement, where the entanglement entropies satisfy area law, and the entanglement spectrum are power-law [12, 22, 30, 31].

In Ref. [32], the authors use the sensitivity of the single-particle eigenenergies to the choice of periodic or antiperiodic boundary conditions as a criterion to identify AL phase. In Ref. [33], a similar criterion is presented to probe the MBL phase. The authors find that the distributions of the off-diagonal matrix elements of a local operator are distinct between the ergodic and MBL systems. Thus, It is natural to ask that how do the eigenstates respond to the change of boundary conditions in both localized and delocalized systems.

In this paper, we investigate the responses of eigenstates with respective to the change of boundary conditions in the localized and delocalized systems. By calculating the overlaps of the corresponding eigenstates between two two different boundary conditions, we find that the eigenstates of the MBL and AL systems

* hfan@iphy.ac.cn

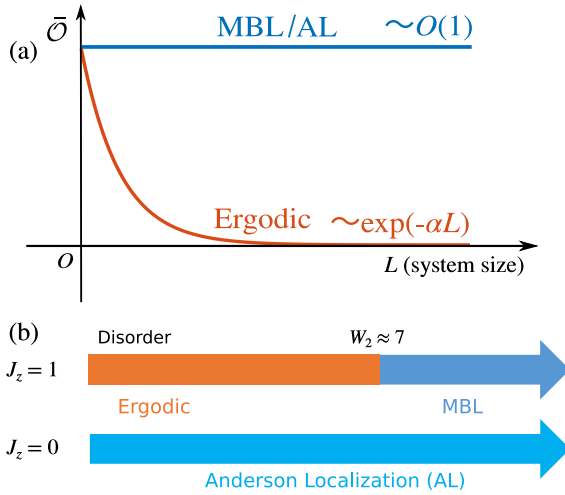


FIG. 1. (a) The scaling functions of $\bar{\mathcal{O}}$ for ergodic, AL and MBL phases, respectively. (b) The phase diagram of Hamiltonian (1). Here, the Hamiltonian is defined by Pauli matrices rather than spin- $\frac{1}{2}$ operators, so the disorder strength W is twice as large relative to the Ref. [11].

show strong robustness, since the eigenstate overlaps are nearly size-independent. Nevertheless, in the ergodic phase, the eigenstate overlaps decay exponentially with the increase of system size, which can be considered as a butterfly effect of the quantum chaos. These results are summaries in Fig. 1(a). In addition, we find that the responses of many-particle eigenstates to the change of boundary conditions in the MBL systems is akin to the one of single-particle eigenstates in AL systems. Thus, we suppose that the eigenstates of the MBL systems are independent of each other, which is distinct to AL systems, whose many-particle eigenstates are Slater determinants. We also demonstrate that this is consistent with the existence of a large number of quasi-local integrals of motion.

The remainder of this paper is organized as follows: In Sec. II, we introduce 1D spin- $\frac{1}{2}$ XXZ model with z -directed random field, and the corresponding phase diagrams are reviewed. We also present the main methods of this paper. The numerical results are shown in Sec. III. In Sec. IV, we give a phenomenological discussion about our results. Finally, in Sec V, we summarize our results and present the outlooks of the future researches. Additional numerical results are present in the Appendices.

II. MODEL AND METHODS

In this section, we introduce the random-field XXZ chain, the main model studied in this paper, and then provide the numerical methods. For our methods, the eigenstate overlaps \mathcal{O} with respective to the different boundary conditions are defined, and this can be considered as the measurement of the response of the eigenstates with respect to the change of the boundary conditions.

A. Model

We consider the spin- $\frac{1}{2}$ XXZ chain with z -directed random field. The Hamiltonian of this model reads

$$\hat{H} = J \sum_i^L (\hat{\sigma}_i^x \hat{\sigma}_{i+1}^x + \hat{\sigma}_i^y \hat{\sigma}_{i+1}^y) + J_z \sum_i^{L-1} \hat{\sigma}_i^z \hat{\sigma}_{i+1}^z + \sum_{i=1}^L h_i \hat{\sigma}_i^z, \quad (1)$$

where $\hat{\sigma}^\alpha$ s ($\alpha = x, y, z$) are Pauli matrices. The random field $h_i \in [-W, W]$ satisfying an uniform distribution. The localization-delocalization transition of this model has been studied extensively in Refs. [9, 24, 25, 31, 33].

By Jordan-Wigner transformation, Hamiltonian (1) can be mapped to a local spinless fermionic system with nearest-neighbor hopping strength J and density-density interaction strength J_z . Below, for convenience, we set $J = 1$. When $J_z = 0$, it is a free system with a disorder potential, and in this case, all the single-particle eigenstates are localized when $W \neq 0$, i.e., it is in AL phase. When $J_z \neq 0$, this becomes an interacting model, where the single-particle description may fail. For different disorder strengths, this system can be divided into three regimes: at weak disorder ($0 < W < W_1$), it belongs to the ergodic phase with all of the eigenstates ergodic, at strong disorder ($W > W_2$), it belongs to MBL phase with all of the eigenstates localized, and at intermediate disorder strength ($W_1 < W < W_2$), the system has many-body mobility edges and is in Griffiths phase [34–36]. Especially, when $J_z = 1$, i.e., the Hamiltonian is Heisenberg coupling, the critical disorder strengths are $W_1 \approx 4$ and $W_2 \approx 7$, respectively [11, 33–36].

B. Methods

Here, we focus on the sensitivity of many-body wave functions with respect to the boundary conditions. We choose periodic boundary condition, i.e., $\hat{\sigma}_{L+1} = \hat{\sigma}_1$, and

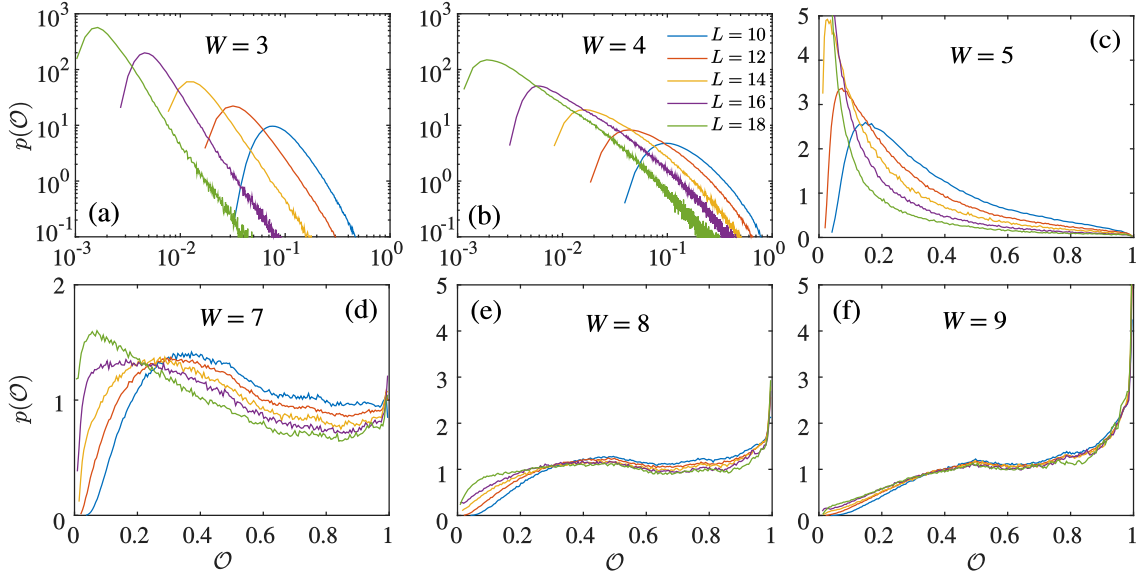


FIG. 2. The distribution of eigenstate overlaps across a MBL transition for different system sizes with $J_z = 1$. (a-c) For weak disorder ($W = 3, 4, 5$), the system is in the ergodic phase. When increasing the system size, the curves of $p(\mathcal{O})$ has an exponentially top-left shift. (d) In the case of critical point ($W = 7$), the top-left shifts almost vanish. (e-f) For strong disorder ($W = 8, 9$), the systems are in the MBL phase. In this case, the curves of $p(\mathcal{O})$ for different system sizes are almost coincide.

anti-periodic boundary condition, i.e., $\hat{\sigma}_{L+1} = -\hat{\sigma}_1$. To quantify the robustness of many-body wave functions, we define the overlaps between two corresponding eigenstates with different boundary conditions

$$\mathcal{O}_n = |\langle \psi_n^p | \psi_n^{ap} \rangle|^2, \quad (2)$$

where $|\psi_n^p\rangle$ and $|\psi_n^{ap}\rangle$ are the eigenstates of \hat{H} with periodic and anti-periodic boundary conditions, respectively. Generally, the change of boundary condition can be regarded as applying a local perturbation. Therefore, according to the perturbation theory, $\sqrt{\mathcal{O}_n}|\psi_n^p\rangle$ is the zero-order contribution (the phase is neglected) of $|\psi_n^{ap}\rangle$, and vice versa. If the eigenstates of the system is robust to the boundary conditions, then the eigenstate overlap \mathcal{O} will be large, i.e., \mathcal{O} can reflect the sensitivity of eigenstates with respect to the boundary conditions.

In addition, we can define the distribution density of

	$L = 10$	$L = 12$	$L = 14$	$L = 16$	$L = 18$
$J_z = 1, W < 6$	30000	10000	1000	300	100
$J_z = 1, W \geq 6$	60000	20000	2000	600	200
$J_z = 0$	60000	20000	2000	600	200

TABLE I. The numbers of disorder averaging for different parameters of Hamiltonian (1).

\mathcal{O}_n as

$$p(\mathcal{O}) \equiv \frac{1}{\mathcal{N}} \sum_{n=1}^{\mathcal{N}} \delta(\mathcal{O}_n - \mathcal{O}), \quad (3)$$

where \mathcal{N} is the number of eigenstate pairs. The means of \mathcal{O}_n can also be obtained as

$$\bar{\mathcal{O}} \equiv \frac{1}{\mathcal{N}} \sum_{n=1}^{\mathcal{N}} \mathcal{O}_n = \int_0^1 d\mathcal{O} \mathcal{O} p(\mathcal{O}). \quad (4)$$

Thus, we can use $\bar{\mathcal{O}}$ to analyze the robustness of eigenstates, quantitatively.

We use exact diagonalization to extract the eigenstates of the random-field XXZ Hamiltonian (1) with periodic and anti-periodic boundary conditions, respectively. For each diagonalization, two boundary conditions should satisfy the same disorder configuration, and due to the spin $U(1)$ symmetry, we only consider the eigenstates with half filling. Nevertheless, it is hard to judge which two eigenstates with different boundary conditions are related. Thus, for each eigenstate $|\psi_n^p\rangle$, we need to calculate the overlaps with all eigenstates of \hat{H} with anti-periodic boundary condition. We regard the maximum among these overlaps as \mathcal{O}_n , i.e.,

$$\mathcal{O}_n = \max\{|\langle \psi_n^p | \psi_1^{ap} \rangle|^2, |\langle \psi_n^p | \psi_2^{ap} \rangle|^2, \dots, |\langle \psi_n^p | \psi_{\mathcal{D}}^{ap} \rangle|^2\}, \quad (5)$$

where $\mathcal{D} = \binom{L}{L/2}$ is the dimension of half-filling Hilbert space.

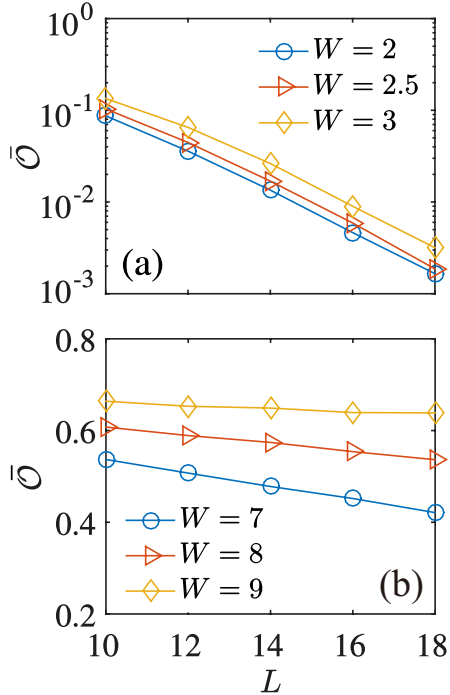


FIG. 3. The scaling of $\bar{\mathcal{O}}$ for different phases. (a) In the ergodic phase, $\bar{\mathcal{O}}$ is exponential decay with the increase of systems sizes. (b) In the MBL phase, $\bar{\mathcal{O}}$ almost keeps invariant, when increasing the system size.

To avoid any possible affection, such as many-body mobility edges, we focus on the middle one eighth of full eigenstates. In this case, the Griffiths phase at intermediate disorder strength can be neglected, and the MBL transition occurs at $W \approx 7$ with $J_z = 1$ [9]. The phase diagrams of the Hamiltonian (1) are presented in Fig. 1(b). The numbers of disorder averaging for different sizes and disorder strengths is presented in Tab. I.

III. NUMERICAL RESULTS

Firstly, we consider the interacting system with $J_z = 1$, i.e., the Hamiltonian is Heisenberg coupling. As mentioned, in this case, the localization-delocalization phase transition point is at $W_2 \approx 7$. In Fig. 2, we show the distribution density of eigenstate overlaps $p(\mathcal{O})$ with different system sizes in both delocalized and localized phases. As the increase of disorder strength, the curves of $p(\mathcal{O})$ have a right shift, which indicate that the robustness of the eigenstates becomes stronger when increasing the disorder strength. Additionally, when increasing the system size, $p(\mathcal{O})$ exhibits an top-left shift in delocalized phase, see Fig 2(a-c). In Fig. 2(d), we can find that this

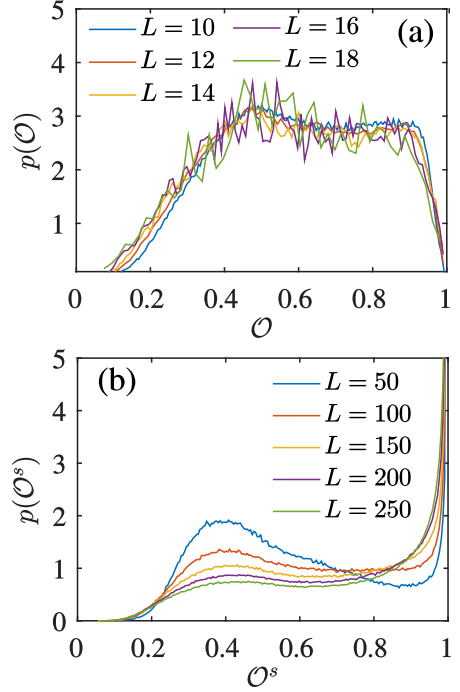


FIG. 4. (a) The distribution of the overlaps of many-body wave functions with respect to the periodic and anti-periodic boundary conditions for H with $J_z = 0$. Here, the system is in AL phase. (b) The distribution of the overlaps of single-particle eigenstates with respect to the periodic and anti-periodic boundary conditions for \hat{H}_F with $W = 0.5$. Here, all of the single-particle eigenstates for each system are considered.

shift almost vanishes near the critical point. In the MBL phase, $p(\mathcal{O})$ is almost size-independent, since the curves of $p(\mathcal{O})$ for different system sizes are nearly coincide, see Fig 2(e,f).

To extract the scaling of the eigenstate overlaps, we calculate the the means of \mathcal{O}_n , i.e., $\bar{\mathcal{O}}$. In Fig. 3, we carry out the finite-size scaling analysis of $\bar{\mathcal{O}}$ between the ergodic and MBL phase. For the ergodic systems, see Fig. 3(a), we can find that $\bar{\mathcal{O}}$ is exponentially dependent on the system size

$$\bar{\mathcal{O}}_{\text{Er}} \propto e^{-\alpha L}. \quad (6)$$

This indicates that the many-body wave functions of ergodic systems are very sensitive to the boundary conditions. Thus, in the thermodynamic limit, the eigenstates of the ergodic systems will become completely different when applying a small local perturbations, and this can be considered as a butterfly effect of eigenstates in the ergodic systems.

For MBL phase, according to Fig. 3(b), $\bar{\mathcal{O}}$ is almost

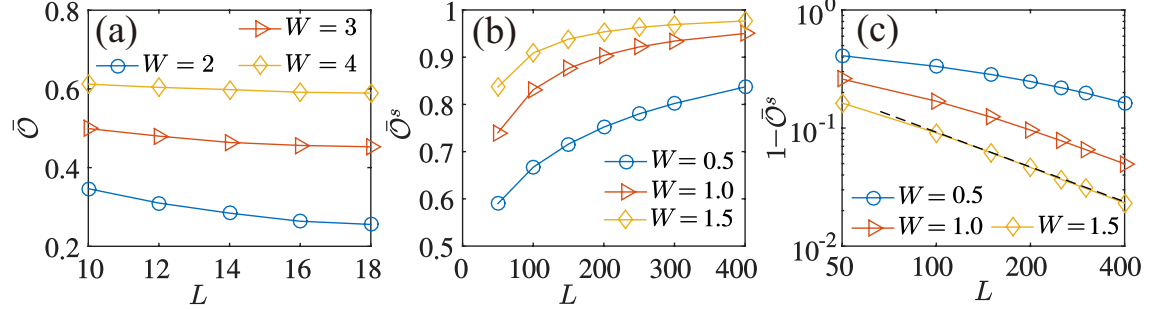


FIG. 5. The scaling of (a) $\bar{\mathcal{O}}$, (b) $\bar{\mathcal{O}}^s$ and (c) $1 - \bar{\mathcal{O}}^s$ for AL systems, respectively. For (c), the black dashed line is a linear fitting, which represents $1 - \bar{\mathcal{O}}^s \propto L^{-1}$.

size-independent

$$\bar{\mathcal{O}}_{\text{MBL}} \propto O(1). \quad (7)$$

Therefore, the many-body wave functions in MBL systems are robust with respect to the boundary conditions.

Now we take up the non-interacting systems, where $J_z = 0$. In this case, the systems are in AL phase for arbitrary weak disorder. In Fig. 4(a), we show the distribution of the eigenstate overlaps of this system. Comparing with Figs. 2(e,f), we find that the curves of $p(\mathcal{O})$ in AL phase are distinct from the MBL phase.

To further uncover the properties of many-particle eigenstates in AL system, we use the single-particle representation to study this system. The Hamiltonian here can be mapped to a free spinless fermion system with Hamiltonian

$$\hat{H}_F = \sum_i^L (\hat{c}_i^\dagger \hat{c}_{i+1} + \hat{c}_{i+1}^\dagger \hat{c}_i) + \sum_{i=1}^L h_i \hat{c}_i^\dagger \hat{c}_i, \quad (8)$$

where \hat{c}_i^\dagger (\hat{c}_i) is the creation (annihilation) operators of fermions. In Fig. 4(b), we present the corresponding distribution of single-particle wave functions \mathcal{O}^s . We can find that the curves of $p(\mathcal{O}^s)$ of \hat{H}_F is similar to the curves of $p(\mathcal{O})$ in MBL systems shown in Figs. 2(e,f).

In addition, we calculate the the means of the overlaps for both many-body wave functions and single-particle wave functions in AL systems, see Fig. 4(a,b). We find they are both almost size-independent

$$\bar{\mathcal{O}}_{\text{AL}}, \bar{\mathcal{O}}_{\text{AL}}^s \propto O(1), \quad (9)$$

showing the robustness of both many-body and single-particle eigenstates to the boundary conditions, which is identified with the MBL systems.

IV. PHENOMENOLOGICAL DISCUSSION

In last section, we have presented the main numerical results. Here, based on these numerical results, we give some phenomenological interpretations. We demonstrate that the fragility of many-body eigenstates in the ergodic systems is consistent with the random matrix theory, and the independence of many-body eigenstates in the MBL systems is consistent with the existence of a large number of quasilocal integrals of motion.

A. Delocalized Systems

We know that the ergodic systems, as a quantum chaos, can be described by the random matrix theory. According to the random matrix theory, the spectrum of the ergodic systems satisfy Wigner-Dyson distribution, and the eigenstates are very sensitive to small perturbations [37, 38]. This sensitivity of many-body wave functions in the ergodic systems can indeed be represented by our results shown in the last section.

Now we analyze the scaling of $\bar{\mathcal{O}}_{\text{Er}}$ by means of perturbation theory and random matrix theory, qualitatively. The difference between the periodic and anti-periodic boundary conditions is a local perturbation V . According to the first-order perturbation theory, we have

$$|\psi_n^{\text{ap}}\rangle = |\psi_n^{\text{p}}\rangle + \sum_{m \neq n} C_{mn} |\psi_m^{\text{p}}\rangle, \quad (10)$$

where $C_{mn} \equiv V_{mn}/(E_n^{\text{p}} - E_m^{\text{p}})$, $V_{mn} \equiv \langle \psi_m^{\text{p}} | V | \psi_n^{\text{p}} \rangle$ and E_n^{p} is the corresponding eigenenergy of $|\psi_n^{\text{p}}\rangle$. In the ergodic phase, using Srednicki's ansatz [39], we have the off-diagonal matrix elements of local operator

$$V_{mn} = e^{-S(E, L)/2} f(E_m, E_n) R_{mn}, \quad (11)$$

where $S(E, L)$ is the statistical entropy at energy $E = (E_n + E_m)/2$, R_{mn} is a random matrix with order one,

and f is a smooth function. Generally, $S(E, L) = \varepsilon \ln \mathcal{D}$ with $\varepsilon \leq 1$. Thus, $|C_{mn}|^2 \propto \mathcal{D}^{-\varepsilon}$, and $\sum_{m=1}^{\mathcal{D}} |C_{mn}|^2 \propto \mathcal{D}^{1-\varepsilon}$. Therefore, for the ergodic systems, $\mathcal{O}_n \propto \mathcal{D}^{\varepsilon-1}$, which indicates $\bar{\mathcal{O}}_{\text{Er}}$ decays exponentially with the increase of the system size.

B. Localized Systems

For AL systems, the single-particle eigenstates satisfy $\bar{\mathcal{O}}_{\text{AL}}^s \propto 1 - c/L$, see Fig. 4(e). Thus, for the many-body eigenstates, which can be written as the Slater determinants, we have $\bar{\mathcal{O}}_{\text{AL}} \sim (1 - c/L)^L \sim O(1)$.

Comparing MBL with AL systems, we find that the behaviors of half-filling eigenstates in MBL phase are more similar to the single-particle rather than many-body eigenstates of AL phase. In fact, this is consistent with the existence of quasilocal integrals of motion in MBL systems. In AL phase, the single-particle eigenstates are local conservation modes, and different modes are decoupled. Thus, the many-body eigenstates, as the Slater determinants, are not independent of each other. In contrast, for the MBL systems, there exist a large number of quasilocal integrals of motion, which are the many-body modes and independent of each other. Therefore, it is reasonable that the many-body eigenstates for the MBL systems behave more likely to the single-particle one in AL systems.

To further illustrate our results, in Appendix A, we study the transverse field Ising model with disorder at longitudinal field. The numerical results of this model is consistent with above discussions, which indicates the universality of our results for different models.

V. CONCLUSION

In summary, we have studied the sensitivities of the eigenstates to the boundary conditions between the localized and delocalized systems. By calculating the overlaps of the corresponding eigenstates between periodic and anti-periodic boundary conditions, we find that the eigenstates are robust to the boundary conditions in the localized phases, while they are fragile in delocalized phases. Furthermore, the many-body eigenstates in the MBL systems have similar behaviors to the single-particle eigenstates in AL system, and this is consistence with the existence of a large number of quasilocal integrals of motion in the MBL phase. Our results provide a new method to diagnose the MBL

phase from the viewpoint of many-body eigenstates. Finally, there remains an open problem as to whether our results are related to the nontrivial dynamics of the MBL systems, such as logarithmic spreading of entanglement entropy.

ACKNOWLEDGMENTS

This work was supported by National Key R & D Program of China (Grant Nos. 2016YFA0302104 and 2016YFA0300600), National Natural Science Foundation of China (Grant Nos. 11774406 and 11934018), Strategic Priority Research Program of Chinese Academy of Sciences (Grant No. XDB28000000), and Beijing Academy of Quantum Information Science (Grant No. Y18G07).

Appendix A: Mixed Transverse Field Ising Model

Here we study another spin model, i.e., the transverse field Ising model with disorder at longitudinal field, to further illustrate our results. The corresponding Hamiltonian reads

$$\hat{H}_{\text{MI}} = \sum_i^L \hat{\sigma}_i^z \hat{\sigma}_{i+1}^z + h_x \sum_{i=1}^L \hat{\sigma}_i^x + \sum_{i=1}^L h_{z,i} \hat{\sigma}_i^z, \quad (\text{A1})$$

where the z -directional random-field $h_{z,i} \in [-W + \bar{h}_z, W + \bar{h}_z]$ satisfying an uniform distribution. Here, we choose the parameters $h_x = 1.05$ and $\bar{h}_z = 0.5$. According to Ref. [40], the critical point of localization-delocalization phase transition is $W = 4.2$. At weak disorder regime ($W < 4.2$), the system is in the ergodic phase. At strong disorder regime ($W > 4.2$), it is in the MBL phase.

Following the numerical method mentioned in main text, we calculate the eigenstates overlaps \mathcal{O} with respect to the periodic and antiperiodic boundary conditions. In Fig. 6, we present the distributions of the eigenstates overlaps, i.e., $p(\mathcal{O})$. In the ergodic phase, we can find that $p(\mathcal{O})$ has a exponential top-left shift with the increase of system size, see Figs. 6(a,b). According to Figs. 6(c,d), in the MBL case, $p(\mathcal{O})$ are almost size-independent, and the curves of $p(\mathcal{O})$ are also similar to the single-particle cases of AL systems shown in Fig. 4(b). Therefore, comparing with Fig. 2, we can find that the numerical results of Hamiltonian (A1) are closely consistent with the cases of the random-field XXZ chain.

[1] J. M. Deutsch, *Phys. Rev. A* **43**, 2046 (1991).

[2] M. Srednicki, *Phys. Rev. E* **50**, 888 (1994).

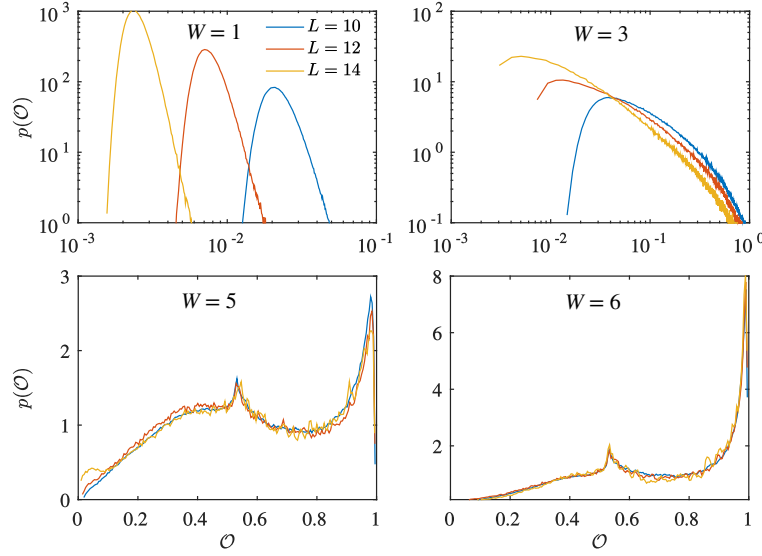


FIG. 6. The distribution of eigenstate overlap in the delocalized and localized systems of Hamiltonian (A1) for different system sizes. (a,b) For weak disorder ($W = 1, 3$), the system is in the ergodic phase. When increasing the system size, the curves of $p(\mathcal{O})$ shift exponentially to top-left. In addition, the curves of $p(\mathcal{O})$ here is similar to the case of the random-field XXZ model showing in Figs. 2(a-c). (c,d) For strong disorder ($W = 5, 6$), the systems are in the MBL phase. In this case, the curves of $p(\mathcal{O})$ for different system sizes are nearly coincide, and they are also consistent with the MBL phases of the random-field XXZ model. Here, the numbers of disorder averaging are 10000, 1000 and 300, when $L = 10, 12, 14$, respectively. In addition, only the middle one eighth of full eigenstates are considered.

- [3] M. Rigol, V. Dunjko, and M. Olshanii, *Nature (London)* **452**, 854 (2008).
- [4] L. D’Alessio, Y. Kafri, A. Polkovnikov, and M. Rigol, *Adv. Phys.* **65**, 239 (2016).
- [5] C. Gogolin and J. Eisert, *Rep. Prog. Phys.* **79**, 056001 (2016).
- [6] R. Nandkishore and D. A. Huse, *Annu. Rev. Condens. Matter Phys.* **6**, 15 (2015).
- [7] P. W. Anderson, *Phys. Rev.* **109**, 1492 (1958).
- [8] D. M. Basko, I. L. Aleiner, and B. L. Altshuler, *Ann. Phys.* **321** (2006).
- [9] V. Oganesyan and D. A. Huse, *Phys. Rev. B* **75**, 155111 (2007).
- [10] I. V. Gornyi, A. D. Mirlin, and D. G. Polyakov, *Phys. Rev. Lett.* **95**, 206603 (2005).
- [11] A. Pal and D. A. Huse, *Phys. Rev. B* **82**, 174411 (2010).
- [12] D. A. Huse, R. Nandkishore, and V. Oganesyan, *Phys. Rev. B* **90**, 174202 (2014).
- [13] E. Altman, *Nat. Phys.* **14**, 979 (2018).
- [14] D. A. Abanin, E. Altman, I. Bloch, and M. Serbyn, *Rev. Mod. Phys.* **91**, 021001 (2019).
- [15] M. Schreiber, S. S. Hodgman, P. Bordia, H. P. Lüschen, M. H. Fischer, R. Vosk, E. Altman, U. Schneider, and I. Bloch, *Science* **349**, 842 (2015).
- [16] J.-y. Choi, S. Hild, J. Zeiher, P. Schauß, A. Rubio-Abadal, T. Yefsah, V. Khemani, D. A. Huse, I. Bloch, and C. Gross, *Science* **352**, 1547 (2016).
- [17] P. Bordia, H. P. Lüschen, S. S. Hodgman, M. Schreiber, I. Bloch, and U. Schneider, *Phys. Rev. Lett.* **116**, 140401 (2016).
- [18] G. A. Álvarez, D. Suter, and R. Kaiser, *Science* **349**, 846 (2015).
- [19] J. Smith, A. Lee, P. Richerme, B. Neyenhuis, P. Hess, P. Hauke, M. Heyl, D. Huse, and C. Monroe, *Nat. Phys.* **12**, 907 (2016).
- [20] K. Xu, J.-J. Chen, Y. Zeng, Y.-R. Zhang, C. Song, W. Liu, Q. Guo, P. Zhang, D. Xu, H. Deng, K. Huang, H. Wang, X. Zhu, D. Zheng, and H. Fan, *Phys. Rev. Lett.* **120**, 050507 (2018).
- [21] Q. Guo, C. Cheng, Z.-H. Sun, Z. Song, H. Li, Z. Wang, W. Ren, H. Dong, D. Zheng, Y.-R. Zhang, R. Mondaini, H. Fan, and H. Wang, [arXiv:1912.02818](https://arxiv.org/abs/1912.02818).
- [22] M. Serbyn, Z. Papić, and D. A. Abanin, *Phys. Rev. Lett.* **111**, 127201 (2013).
- [23] L. Rademaker and M. Ortúñ, *Phys. Rev. Lett.* **116**, 010404 (2016).
- [24] J. H. Bardarson, F. Pollmann, and J. E. Moore, *Phys. Rev. Lett.* **109**, 017202 (2012).
- [25] M. Serbyn, Z. Papić, and D. A. Abanin, *Phys. Rev. Lett.* **110**, 260601 (2013).
- [26] H. Kim and D. A. Huse, *Phys. Rev. Lett.* **111**, 127205 (2013).
- [27] C. W. J. Beenakker, *Rev. Mod. Phys.* **69**, 731 (1997).
- [28] R. Nandkishore, S. Gopalakrishnan, and D. A. Huse, *Phys. Rev. B* **90**, 064203 (2014).
- [29] W. Buijsman, V. Cheianov, and V. Gritsev, *Phys. Rev. Lett.* **122**, 180601 (2019).
- [30] J. Z. Imbrie, *J. Stat. Phys.* **163**, 998 (2016).

- [31] M. Serbyn, A. A. Michailidis, D. A. Abanin, and Z. Papić, *Phys. Rev. Lett.* **117**, 160601 (2016).
- [32] J. T. Edwards and D. J. Thouless, *J. Phys. C* **5**, 807 (1972).
- [33] M. Serbyn, Z. Papić, and D. A. Abanin, *Phys. Rev. X* **5**, 041047 (2015).
- [34] K. Agarwal, S. Gopalakrishnan, M. Knap, M. Müller, and E. Demler, *Phys. Rev. Lett.* **114**, 160401 (2015).
- [35] C. L. Bertrand and A. M. García-García, *Phys. Rev. B* **94**, 144201 (2016).
- [36] M. Serbyn, Z. Papić, and D. A. Abanin, *Phys. Rev. B* **96**, 104201 (2017).
- [37] T. A. Brody, J. Flores, J. B. French, P. A. Mello, A. Pandey, and S. S. M. Wong, *Rev. Mod. Phys.* **53**, 385 (1981).
- [38] L. D'Alessio, Y. Kafri, A. Polkovnikov, and M. Rigol, *Advances in Physics* **65**, 239 (2016).
- [39] M. Srednicki, *J. Phys. A* **32**, 1163 (1999).
- [40] S. Sahu, S. Xu, and B. Swingle, *Phys. Rev. Lett.* **123**, 165902 (2019).